INTERNATIONAL JOURNAL OF COMPUTERS COMMUNICATIONS & CONTROL
Online ISSN 1841-9844, ISSN-L 1841-9836, Volume: 20, Issue: 2, Month: April, Year: 2025
Article Number: 6896, https://doi.org/10.15837/ijccc.2025.2.6896

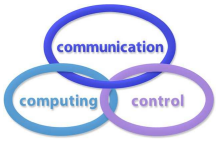

CCC Publications

State-of-Charge Estimation of an Experimentally Identified Lithium-ion Cell Model using Advanced Nonlinear Filters

S. Gupta, A. K. Naik, R. Dey, A. K. Singh, M. Popa, A. Popa

Shivam Gupta
Department of Electrical Engineering
National Institute of Technology Silchar
Silchar, 788010, Assam, India
shivamgpt66@gmail.com

Amit Kumar Naik*
Department of Electrical Engineering
Indian Institute of Technology Indore
Indore, 453552, Madhya Pradesh, India
*Corresponding author: phd1901102027@iiti.ac.in

Rajeeb Dey*
Department of Electrical Engineering
National Institute of Technology Silchar
Silchar, 788010, Assam, India
*Corresponding author: rajeeb@ee.nits.in

Abhinoy Kumar Singh
Department of Electrical Engineering
Indian Institute of Technology Patna
Bihta, 801106, Patna, Bihar, India
abhinoy.singh@iitp.ac.in

Mihaela Popa*
1. Petroleum-Gas University of Ploiesti, Romania
2. Aurel Vlaicu University of Arad, Romania
*Corresponding author: mihaela2popa@yahoo.com

Alexandru Popa
Faculty of Engineering
Aurel Vlaicu University of Arad, Romania
alexpopaarad@yahoo.com

Abstract

This paper considers the state-of-charge (SoC) estimation problem for Lithium-ion (Li-ion) cells. An accurate SoC estimation is crucial in many aspects. Firstly, it prolongs battery lifespan by preventing overcharging and overdischarging. Additionally, preventing overcharging, and hence thermal runaway, averts any potential risk of fire or explosion in the battery systems. Understanding the SoC enables the efficient utilization of a battery's capacity, enhancing the performance of the device or vehicle it powers. This is especially crucial for electric vehicles, where concerns about driving range are prevalent. SoC estimation is frequently paired with state-of-health (SoH) estimation to assess the battery's overall condition. This combination aids in forecasting the battery's remaining lifespan and scheduling maintenance or replacement. In grid storage and renewable energy systems, precise SoC estimation aids in balancing energy supply and demand, ensuring dependable and efficient energy management. The above-mentioned discussion highlights the importance of the study which is carried out in this work. The existing works in the literature mainly use the extended Kalman filter (EKF) for the SoC estimation problem. It should be noted that the performance of the EKF degrades as the system's non-linearity increases. Moreover, the existing battery management systems are complex and inherently involve high nonlinearities which further extend as these systems are expanded. For these reasons, the EKF may lose its applicability for applications demanding highly accurate SoC estimates. In this paper, therefore, we apply a more accurate cubature-quadrature Kalman filter (CQKF) to estimate the SoC of the Li-ion cell. The

SoC estimates provided by the CQKF are more accurate than those provided by the EKF. In this regard, we first develop the completely observable equivalent circuit model (ECM) of a Li-ion cell by experimentally identifying the parameters of the cell model. The experimental study is carried out in a commercially available 2.5 Ah lithium iron phosphate (LFP) cell (A123 ANR26650M1-B). Subsequently, we apply the cubature quadrature Kalman filter (CQKF) for estimating the SoC of the considered Li-ion cell. We also perform a comparative analysis of the CQKF and the extended Kalman filter (EKF) based SoC estimation for the considered model. We further extended the analysis for the missing measurement case, where the actual measurement is intermittently lost or does not contain sufficient information for the state measurement. The efficacy of the estimation schemes is validated both experimentally and in simulation by computing several performance indexes. The simulation results show that, compared with the EKF, the implementation of the CQKF improves the SoC estimation accuracy significantly.

Keywords: Cubature quadrature Kalman filter, extended Kalman filter, lithium-ion cell, state of charge estimation.

1 Introduction

Electric vehicle (EV) technology is gaining popularity as a result of its lower emissions compared with internal combustion (IC) engine-based vehicles. EV technology is widely regarded as a viable option for reducing global air pollution and carbon footprint. The energy source for EVs is battery. Like conventional batteries, EV batteries are also made up of many single cells coupled in series or parallel to meet the high energy and power demands. The cells are additionally constrained in their operation by voltage, temperature, and current [1, 2]. Therefore, an EV necessitates a battery management system (BMS) to protect, monitor, and control the batteries. Among several key functions of the BMS, one particular function, namely SoC estimation of the li-ion cell, is investigated in this paper.

The SoC level of a Li-ion cell cannot be measured directly as it depends on the concentration of lithium ions at the electrodes [3]. Furthermore, the unideal characteristics of the cells make the SoC estimation of a complete battery pack difficult. In addition, noisy sensor measurements, temperature and battery parameter fluctuations, battery aging, and the overall complicated and nonlinear behavior of batteries are all challenges for accurate SoC estimation.

Generally, the SoC estimation is performed using current-based, voltage-based, and model-based approaches [4]. Current-based approaches estimate SoC by using the 'Coulomb counting' equation, which relates the current drawn from (or supplied to) the battery to its capacity. It is a reliable method of calculating SoC. However, the knowledge of the initial SoC level is to determine the SoC at any subsequent time instant, which is not always attainable. In voltage-based approaches, the relationship between open-circuit voltage (OCV) and short-circuit current (SC) is used. The disadvantage is that for the terminal voltage to achieve OCV, the battery must be properly relaxed. Model-based estimation mathematically relates measurable signals (e.g., terminal voltage) to SoC. It is known to provide accurate and precise estimates and incorporates elements of current and voltage-based estimation techniques [5, 6].

Equivalent circuit models (ECM) use electrical components, such as resistors and capacitors to simulate the electrochemical process of a cell. ECMs are commonly employed in model-based estimation because of their improved accuracy with ease of implementation [7, 8, 9, 10]. In [11] and [12], the authors suggest a composite ECM based on the Shepherd, Unnewher, and Nernst models. Other models are also discussed, including zero-state hysteresis, one-state hysteresis, and enhanced self-correcting (ESC) models. Adding resistor-capacitor (RC) branches to these models improves their accuracy significantly. A comparison of twelve state-of-the-art lumped ECMs, as well as an examination of the model structure and parameter identification can be found in [13]. The second-order RC model has been demonstrated to be the best model for estimating SoC, especially when significant dynamic loads are present [14, 15].

As SoC cannot be directly approximated, the estimation process must rely on available noisy measurements to rebuild the system's internal states. Therefore, it becomes a problem of estimation and filtering [16, 17]. For estimation, the Kalman filter (KF) is a popular mathematical tool that

provides optimal estimates for the linear systems [18]. However, it suffers from poor accuracy for nonlinear systems [19]. Since our problem is inherently nonlinear, it demands a filtering algorithm that can handle the nonlinearities. Various nonlinear extensions of the KF are discussed in the literature [20, 21]. The EKF is implemented in [11, 22] to estimate the SoC of the battery pack. However, the complexity and nonlinearities of BMS are expected to increase considering the advancement in battery technologies. It is well-known that the EKF performs with poor accuracy with increased nonlinearities. Our main objective is to estimate the SoC more accurately. Therefore, we chose CQKF [23] because of its improved accuracy. We compare the performance of the CQKF and EKF on the experimentally identified ECM. The results show that the SoC estimation provided by the CQKF is more accurate compared with the EKF.

Summarizing the above discussion, we now highlight the main contributions of the manuscript as follows

- We address the problem of state-of-charge (SoC) estimation for the Lithium-ion cell, and choose $LiFePO_4$ as the test cell.
- We develop an equivalent circuit model by experimentally calculating parameters' values.
- Subsequently, we propose a state-space model that imitates the dynamics of the considered cell.
- For the newly developed model, we apply the advanced Gaussian filter, *i.e.,* cubature-quadrature Kalman filter to estimate the SoC.
- We validate the improved performance of the proposed method by comparing it with the existing extended Kalman filter-based SoC estimation method.
- We extended the comparison for missing measurement phenomenon.

2 Experimental setup

As illustrated in Fig. 1, the experimental setup comprises of the LiFePO4 (or LFP) cell to be investigated and a PC-based Bitrode FTV storage device testing module. In this experiment, we use A123 ANR26650M1-B and 2.5 Ah LFP cell. however, the actual capacity turned out to be 2.481 Ah. In its low current and high current operating modes, the Bitrode FTV testing module can supply currents up to 6 A and 100 A, respectively. The measurement for the terminal current and voltage is taken with the sampling rate of 1 s while charging and discharging the cell in the low current mode of the testing module. The current and voltage are measured with 1 mA and 1 mV precision, respectively, using the testing module. All the tests are performed at room temperature ∼25°C. The cell parameters are shown in Table 1.

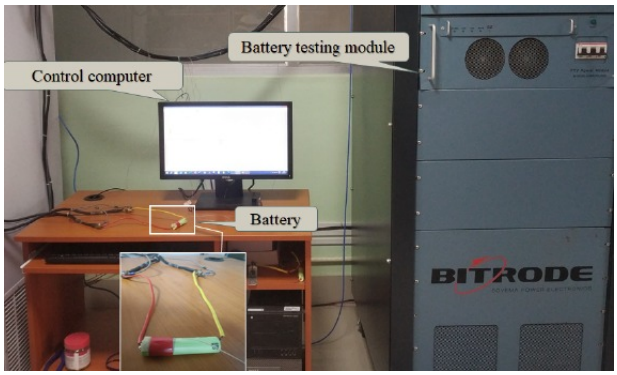

Figure 1: Experimental setup.

Table 1: LFP cell parameters

Parameters	Value
Cell capacity	2.5/2.4 Ah
Nominal voltage	3.3 V
Upper cut off voltage	3.6 V
Lower cut off voltage	2 V
Cycle life at 20 A discharge	>1000 cycles

2.1 Identifying OCV-SoC Relationship

The open-circuit voltage or OCV is the no-load voltage across battery terminals when the battery has attained internal equilibrium. OCV normally increases monotonically as a nonlinear function of SoC. OCV may also depend on cell temperature, but this effect is negligible compared to the effect of SoC [24, 25].

For the given cell to obtain the OCV data, the cell is charged and discharged between the upper cutoff voltage and lower cut-off voltage which in the present case is 3.6 V and 2 V respectively at C/20 rate. Note that cells may follow different OCV-SoC curves during charging and discharging i.e., hysteresis as shown in Fig. 2, but the model considers only the averaged OCV curve shown in Fig. 3. Additionally, the long-term aging of OCV is also neglected.

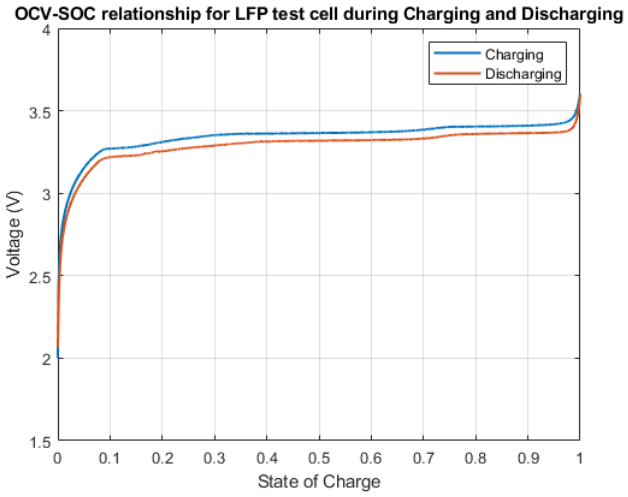

Figure 2: OCV-SoC curves during charging and discharging.

Different cell chemistry exhibit different OCV-SoC relationships, which may have a significant impact on the SoC estimation accuracy. For the LFP cell considered in this work, the curve is found to be flat from 20% to 90% SoC as shown in Fig. 3. Due to this flatness, a small variation in OCV will correspond to a large variation in SoC, which implies that any small noise or disturbance in the voltage measurement will have a large impact on SoC estimation. Hence, for an LFP cell, an accurate and precise voltage measurement is critical.

The electro-chemical models for OCV behaviour in respect of SoC are as follows:

1. Shepherd Model

$$V_T(t) = K_0 - R_0.I\,(t) + \frac{K_1}{z(t)}. \tag{1}$$

2. Unnewehr Universal Model

$$V_T\,(t) = K_0 - R_0.I\,(t) + K_2.z(t). \tag{2}$$

3. Nernst model

$$V_T\,(t) = K_0 - R_0.I\,(t) + K_3 \ln\left(z\,(t)\right)\ + K_4 \ln(1 - z(t))\ . \tag{3}$$

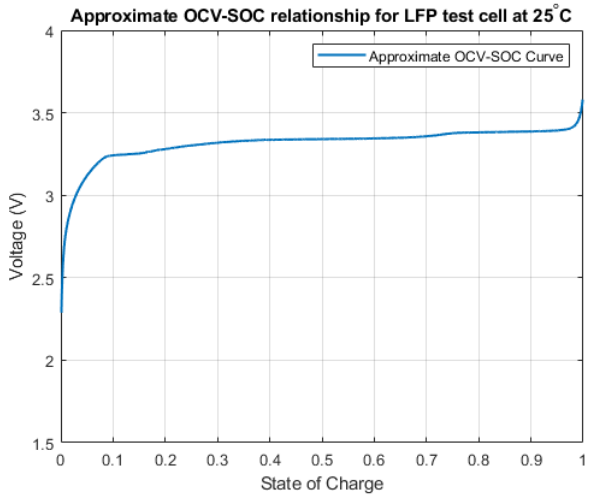

Figure 3: Approximate OCV-SoC curve for LFP cell.

4. Combined Model

$$\begin{aligned} V_T(t) = K_0 - R_0.I(t) + \frac{K_1}{z(t)} + K_2.z(t) \\ + K_3 \ln(z(t)) \ + K_4 \ln(1 - z(t)) \ , \end{aligned} \tag{4}$$

where $V_{OC}(z(t)) = K_0 + \frac{K_1}{z(t)} + K_2.z(t) + K_3 \ln(z(t)) + K_4 \ln(1 - z(t))$ and, $K_0 = 3.552, K_1 = -0.00072, K_2 = -0.2744, K_3 = +0.1372, K_4 = -0.03967$.

Fig. 4 shows the fitted OCV-SoC curve for the LFP test cell using curve fitting tool in MATLAB obtained from the approximated experimental curve shown in Fig. 3.

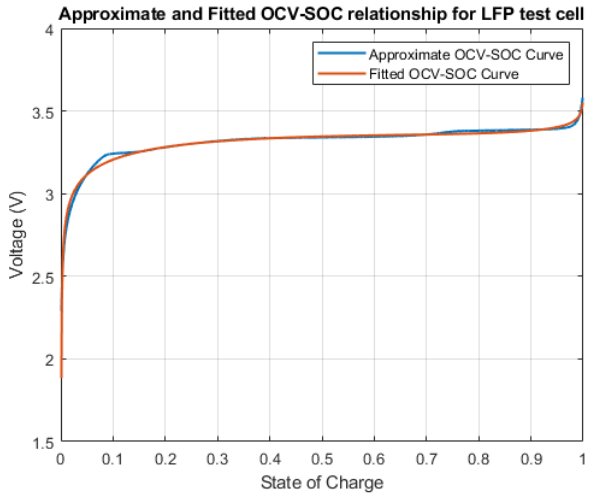

Figure 4: Approximate and Fitted OCV-SoC curve for LPF test cell.

3 State of Charge (SoC) Estimation

In this section, the SoC estimation algorithms are discussed. The discrete-time state space model of the cell are rewritten in the form of

$$\begin{aligned} \mathbf{x}_{k+1} &= f(\mathbf{x}_k, \mathbf{u}_k) \\ \mathbf{y}_{k+1} &= g(\mathbf{x}_{k+1}, \mathbf{u}_k) , \end{aligned} \tag{5}$$

Table 2: Identified parameter values.

Parameters	Value
R_0	$15.788m\Omega$
R_1	$18.155m\Omega$
R_2	$26.196m\Omega$
C_1	$1304.6F$
C_2	$96655F$

where $\mathbf{x}_k = \begin{bmatrix} I_{R_1}[k] & I_{R_2}[k] & z[k] \end{bmatrix}$ is the state vector, $\mathbf{y}_k = V_T[k]$ is the measured terminal voltage, $\mathbf{u}_k = I[k]$ is the measured terminal current, and the functions $f(\cdot)$ and $g(\cdot)$ are the state transition and measurement (or output) functions, respectively, and given by

$$f(\mathbf{x}_k, \mathbf{u}_k) = \begin{bmatrix} e^{-\Delta t/\tau_1}.I_{R_1}[k] + \left(1 - e^{-\Delta t/\tau_1}\right).I[k] \\ e^{-\Delta t/\tau_2}.I_{R_2}[k] + \left(1 - e^{-\Delta t/\tau_2}\right).I[k] \\ z[k] - \frac{\eta \Delta t}{3600.Q} I[k] \end{bmatrix}. \tag{6}$$

$$g(\mathbf{x}_k, \mathbf{u}_k) = V_{OC}(z[k]) - R_1.I_{R_1}[k] - R_2.I_{R_2}[k] - R_0 I[k]. \tag{7}$$

It is worth mentioning at this stage that manufacturing variability and deterioration of the cell chemically and mechanically can potentially contribute to parametric uncertainty [26]. The CQKF is expected to perform better than the EKF under such circumstances.

3.1 Extended Kalman Filter Algorithm

The EKF is a nonlinear extension of KF that handles the nonlinearities in the system model by simply computing the Jacobian at each time step. The state-space equations of a discrete time nonlinear system is given by:

$$\begin{aligned} \mathbf{x}_{k+1} &= f(\mathbf{x}_k, \mathbf{u}_k) + \mathbf{w}_k \\ \mathbf{y}_{k+1} &= g(\mathbf{x}_{k+1}, \mathbf{u}_k) + \mathbf{v}_k, \end{aligned} \tag{8}$$

where $\mathbf{w}_k$ and $\mathbf{v}_k$ represents the process and measurement noises, respectively. Furthermore, it is assumed that $\mathbf{w}_k \sim \mathcal{N}(0, \mathbf{\Sigma}_{w,k})$ and $\mathbf{v}_k \sim \mathcal{N}(0, \mathbf{\Sigma}_{v,k})$ are zero mean white Gaussian noises with covariances $\mathbf{\Sigma}_w$ and $\mathbf{\Sigma}_v$, respectively. Using first-order Taylor series expansion on $f(\cdot)$ and $g(\cdot)$ [11], one can get:

$$f(\mathbf{x}_k, \mathbf{u}_k) = f\left(\hat{\mathbf{x}}_{k-1}^+, \mathbf{u}_k\right) + \left.\frac{\partial f(\mathbf{x}_k, \mathbf{u}_k)}{\partial \mathbf{x}_k}\right|_{\mathbf{x}_k = \hat{\mathbf{x}}_{k-1}^+} \left(\mathbf{x}_k - \hat{\mathbf{x}}_{k-1}^+\right) \tag{9}$$

$$g(\mathbf{x}_k, \mathbf{u}_k) = g\left(\hat{\mathbf{x}}_k^-, \mathbf{u}_k\right) + \left.\frac{\partial g(\mathbf{x}_k, \mathbf{u}_k)}{\partial \mathbf{x}_k}\right|_{\mathbf{x}_k = \hat{\mathbf{x}}_k^-} \left(\mathbf{x}_k - \hat{\mathbf{x}}_k^-\right), \tag{10}$$

where $\mathbf{A}_k = \left.\frac{\partial f(\mathbf{x}_k, \mathbf{u}_k)}{\partial \mathbf{x}_k}\right|_{\mathbf{x}_k = \hat{\mathbf{x}}_{k-1}^+}$ and $\mathbf{C}_k = \left.\frac{\partial g(\mathbf{x}_k, \mathbf{u}_k)}{\partial \mathbf{x}_k}\right|_{\mathbf{x}_k = \hat{\mathbf{x}}_k^-}$. For completeness of the presentation and ease of understanding the summary of the EKF implementation algorithm is summarized below sequentially in terms of the executable equations,

1. *Initialization (to be executed only once):*

$$\hat{\mathbf{x}}_0^+ = \mathbb{E}[\mathbf{x}_0]. \tag{11}$$

$$\mathbf{\Sigma}_{\tilde{x},0}^+ = \mathbb{E}\left[\left(\mathbf{x}_0 - \hat{\mathbf{x}}_0^+\right)\left(\mathbf{x}_0 - \hat{\mathbf{x}}_0^+\right)^T\right]. \tag{12}$$

2. *Prediction step:*
   A priori state estimation

$$\hat{\mathbf{x}}_k^- = f\left(\hat{\mathbf{x}}_{k-1}^+, \mathbf{u}_{k-1}\right). \tag{13}$$

A priori error covariance matrix

$$\mathbf{\Sigma}_{\tilde{x},k}=\mathbf{A}_{k-1}\mathbf{\Sigma}^{+}_{\tilde{x},k-1}\mathbf{A}^{T}_{k-1}+\mathbf{\Sigma}_{w}\ . \tag{14}$$

3. *Correction step:*
Kalman gain

$$\mathbf{L}_k=\mathbf{\Sigma}^{-}_{\tilde{x},k}\mathbf{C}^{T}_{k}\left[\mathbf{C}_k\mathbf{\Sigma}^{-}_{\tilde{x},k}\mathbf{C}^{T}_{k}+\mathbf{\Sigma}_{v}\ \right]^{-1}. \tag{15}$$

A posteriori state estimation

$$\hat{\mathbf{x}}^{+}_{k}=\hat{\mathbf{x}}^{-}_{k}+\mathbf{L}_k\left[\mathbf{y}_k-g\left(\hat{\mathbf{x}}^{-}_{k},\mathbf{u}_k\right)\right]. \tag{16}$$

A posteriori error covariance matrix

$$\mathbf{\Sigma}^{+}_{\tilde{x},k}=(\mathbf{I}-\mathbf{L}_k\mathbf{C}_k)\mathbf{\Sigma}_{\tilde{x},k}\ . \tag{17}$$

The superscript '-' indicates a priori estimate, while the superscript '+' indicates a posteriori estimate. $\hat{\mathbf{x}}^{+}_{0}$ is initial state vector value given by $\left[\begin{array}{ccc} 0 & 0 & 0.9 \end{array}\right]$, $\mathbf{\Sigma}^{+}_{\tilde{x},0}$ is error covariance and it is initialized with value $diag\left(\left[\begin{array}{ccc} 1e-3 & 1e-3 & 1e-3 \end{array}\right]\right)$, $\mathbf{\Sigma}_w$ is process noise covariance and is initialized with value $diag\left(\left[\begin{array}{ccc} 1e-4 & 1e-4 & 0.9e-5 \end{array}\right]\right)$. $\mathbf{\Sigma}_v$ is measurement noise covariance and is initialized with value $2e-2$.

3.2 Cubature Quadrature Kalman Filter (CQKF)

In nonlinear systems, the intractable integrals appear during the filtering process. These integrals can not be solved analytically, and require to be numerically approximated. The cubature Kalman filter (CKF) [20, 21] uses spherical cubature rule to approximate these integrals. The CKF is further generalized in CQKF [27] by increasing the order of Gauss-Laguerre approximation. The quadrature rule's order defines the accuracy of the CQKF. The higher the number of quadrature points, the more accurate the result. However, $2nn'$ support points and weights are needed for the CQKF filter of order n'. Unlike the EKF, the CQKF is derivative free, thus no Jacobian matrix calculation is required. The algorithm of the CQKF could be summarized sequentially as follows [27]:

1. Filter initialization
   - Initialize the filter with $\hat{\mathbf{x}}_{0|0}$ and $\mathbf{P}_{0|0}$.
   - Calculate the CQ points, ξ_j, their corresponding weights w_j $(j=1,2,\cdots,2nn')$.
2. Predictor Step
   - Perform the Cholesky decomposition of posterior error covariance

$$\mathbf{P}_{k|k}=\mathbf{S}_{k|k}\mathbf{S}^{T}_{k|k}. \tag{18}$$

   - Evaluate CQ points

$$\mathbf{X}_{j,k|k}=\mathbf{S}_{k|k}\xi_j+\hat{\mathbf{x}}_{k|k}. \tag{19}$$

   - Update CQ points

$$\mathbf{X}_{j,k+1|k}=\emptyset(\mathbf{X}_{j,k|k}). \tag{20}$$

   - Compute the time updated mean and covariance

$$\hat{\mathbf{x}}_{k+1|k}=\sum_{j=1}^{2nn'}w_j\mathbf{X}_{j,k+1|k}. \tag{21}$$

$$\mathbf{P}_{k+1|k}=\sum_{j=1}^{2nn'}w_j\mathbf{X}_{j,k+1|k}\mathbf{X}^{T}_{j,k+1|k}-\hat{\mathbf{x}}_{k+1|k}\hat{\mathbf{x}}^{T}_{k+1|k}+\mathbf{Q}_k. \tag{22}$$

3. Measurement update

- Perform the Cholesky decomposition of prior error covariance

$$\mathbf{P}_{k+1|k} = \mathbf{S}_{k+1|k}\mathbf{S}_{k+1|k}^{T}. \tag{23}$$

- Evaluate the CQ points

$$\mathbf{X}_{j,k+1|k} = \mathbf{S}_{k+1|k}\xi_j + \hat{\mathbf{x}}_{k+1|k}. \tag{24}$$

- Find the predicted measurements at each CQ points

$$\mathbf{Y}_{j,k+1|k} = \gamma\left(\mathbf{X}_{j,k+1|k}\right). \tag{25}$$

- Estimate the predicted measurement

$$\hat{\mathbf{y}}_{k+1|k} = \sum_{j=1}^{2nn'} w_j \mathbf{Y}_{j,k+1|k}. \tag{26}$$

- Calculate the covariances

$$\mathbf{P}_{y_{k+1},y_{k+1}} = \sum_{j=1}^{2nn'} w_j \mathbf{Y}_{j,k+1|k}\mathbf{Y}_{j,k+1|k}^{T} - \hat{\mathbf{y}}_{k+1|k}\hat{\mathbf{y}}_{k+1|k}^{T} + \mathbf{R}_k. \tag{27}$$

$$\mathbf{P}_{x_{k+1},y_{k+1}} = \sum_{j=1}^{2nn'} w_j \mathbf{X}_{j,k+1|k}\mathbf{Y}_{j,k+1|k}^{T} - \hat{\mathbf{x}}_{k+1|k}\hat{\mathbf{y}}_{k+1|k}^{T}. \tag{28}$$

- Calculate Kalman gain

$$\mathbf{K}_{k+1} = \mathbf{P}_{x_{k+1},y_{k+1}}\mathbf{P}_{y_{k+1},y_{k+1}}^{-1}. \tag{29}$$

- Compute the posterior state values

$$\hat{\mathbf{x}}_{k+1|k+1} = \hat{\mathbf{x}}_{k+1|k} + \mathbf{K}_{k+1}(\mathbf{y}_{k+1} - \hat{\mathbf{y}}_{k+1|k}). \tag{30}$$

- The posterior error covariance matrix is given by

$$\mathbf{P}_{k+1|k+1} = \mathbf{P}_{k+1|k} - \mathbf{K}_{k+1}\mathbf{P}_{y_{k+1},y_{k+1}}\mathbf{K}_{k+1}^{T}. \tag{31}$$

4 Simulation and Results

In this section, the performance of the two estimation algorithms is presented and further illustrated through simulation and experimental studies. A comparison between EKF and CQKF results is shown in Figs. 5-7 when subjected to UDDS profile test. The results are generated with 3^{rd} order quadrature rule for CQKF. $\mathbf{P}_{0|0}$ error covariance and it is initialized with value $diag([\ 1e-3 \quad 1e-3 \quad 1e-3\ ])$. The values of $\mathbf{Q}_k$ and $\mathbf{R}_k$ are selected as $diag([e-4\ \ e-4\ \ 0.9e-5])$ and $2e-2$, respectively. The results are generated with 100 Monte-Carlo runs.

Fig. 5 shows the performance of the EKF and CQKF for SoC estimation on the UDDS profile and as we can see CQKF performance is better as compared to EKF which can be confirmed from the coefficient of determination (R^2) from Table 3. Fig. 6 shows the absolute error for SoC estimation and the mean absolute error for CQKF is less as compared that of EKF, which can be seen in Table 3. Fig. 7 shows the estimated output voltage performance of the EKF and CQKF which shows that both the algorithms perform well for output estimation.

To further validate the model, Dynamic Stress Test (DST) is also performed on a battery in which a series of discharge current pulses are applied to the cell under test at room temperature ∼25℃. Fig. 8 compares the performance of EKF and CQKF for estimating SoC on the DST profile, and we can observe that the CQKF performs better than EKF, as evidenced by the coefficient of determination (R^2) in Table 3. Fig. 9 depicts the absolute error for SoC estimation, and the mean absolute error for

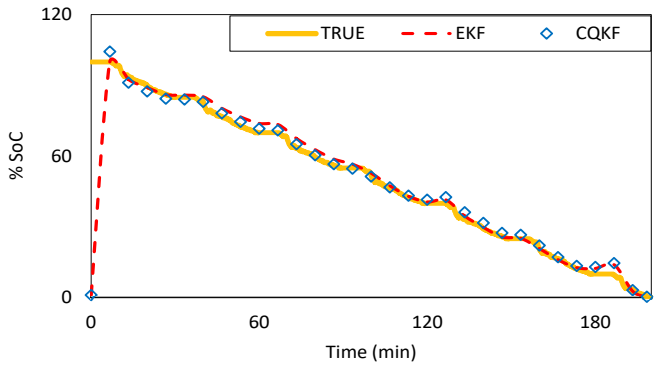

Figure 5: SoC estimation performance of EKF and CQKF using UDDS profile.

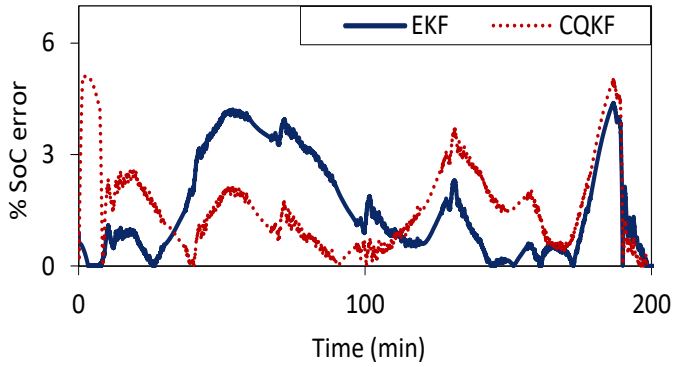

Figure 6: Absolute state estimation error of EKF and CQKF using UDDS profile.

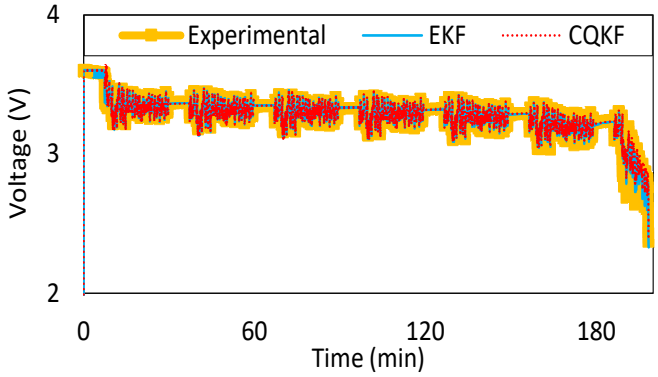

Figure 7: Output voltage performance of EKF and CQKF using UDDS profile.

Table 3: Analysis of SoC estimation for EKF and CQKF.

Filter	**Drive Cycle**	$R^2(-)$	**MAE(%)**	**RMSE(%)**
EKF	UDDS	0.9947	1.5984	2.0873
	DST	0.9900	1.8624	2.7227
CQKF	UDDS	0.9956	1.4982	1.9250
	DST	0.9955	1.4756	1.8368

Table 4: Analysis of terminal voltage for EKF and CQKF.

Filter	**Drive Cycle**	$R^2(-)$	**MAE(mV)**	**RMSE(mV)**
EKF	UDDS	0.9184	8.7696	35.7395
	DST	0.8876	8.5669	33.8187
CQKF	UDDS	0.9073	10.8067	38.1114
	DST	0.8784	10.0836	35.1800

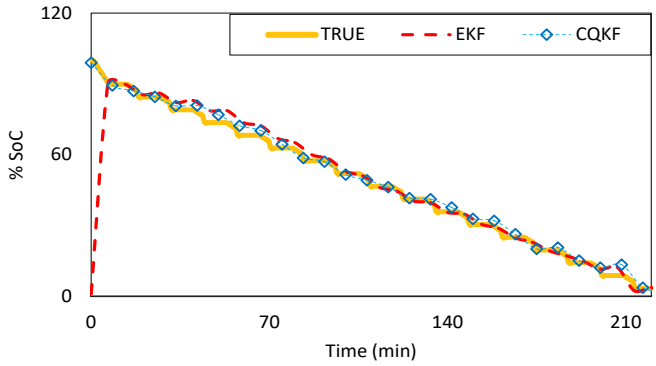

Figure 8: SoC estimation performance of EKF and CQKF using DST profile.

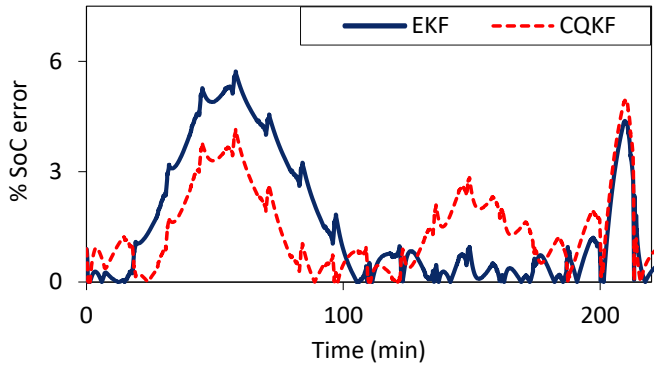

Figure 9: Absolute state estimation error of EKF and CQKF using DST profile.

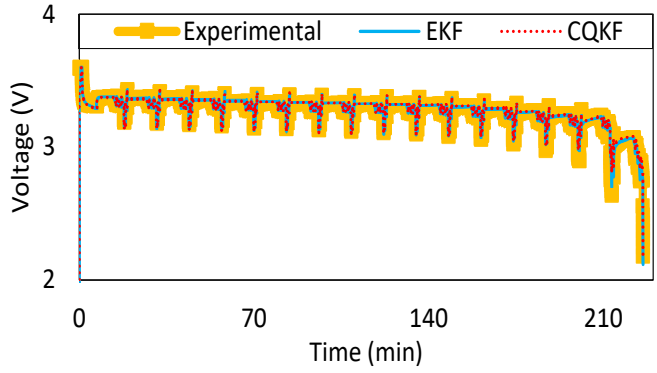

Figure 10: Output voltage performance of the EKF and CQKF using DST profile.

CQKF is lower than that for EKF, as shown in Table 3. The estimated output voltage performance of the EKF and CQKF is shown in Fig. 10, demonstrating that both algorithms perform well for output estimation.

To conduct the statistical analysis of the overall performance of two algorithms, a few performance indices are shown in Table 3 and 4. The indices are calculated for both the model output and the predicted SoC, with the former being compared to the measured voltage and the latter being compared to the theoretical SoC computed using the coulomb counting technique [28].

It should be noted that the batteries inherently contain complex structure, which is often influenced by various factors. In such complex environment, the received measurements are often corrupted. Specifically, the measurement is not received for many time-instants or the received measurement does not carry sufficient information for the state estimation. This phenomenon is called missing measurement. The EKF and CQKF are incapable to handle the missing measurements phenomenon in their conventional form. Therefore, these filtering algorithms are required to be rederived to handle the missing measurements. Further, note that the measurement equation (Eq. (5)) does not include the missing measurement phenomenon and is required to modified. The proposed measurement equation incorporating the missing measurements possibility is given as

$$\mathbf{z}_{k+1} = \boldsymbol{\beta} g\left(\mathbf{x}_{k+1}, \mathbf{u}_k\right), \tag{32}$$

where $\mathbf{z}_{k+1}$ represents missing measurement and $\boldsymbol{\beta}$ is a Bernoulli random variable incorporating the missing measurement possibilities: $\boldsymbol{\beta} = 1$ represents that the measurement is received while $\boldsymbol{\beta} = 0$ denotes that the corresponding measurement is lost.

Following the above discussion, we modified the EKF and the CQKF for Eq. (32) and compared the different indices considered in the paper. It should be noted that the missing measurement probability is not very high in general for any system. Subsequently, we consider that only 10% of total measurement are lost for the system. Alternatively, the missing measurement probability is considered as 0.1. Tables 5 and 6 compares the different indices for the modified CQKF and EKF, which concludes that the modified CQKF for missing measurements performs better than the modified EKF for the missing measurement.

Table 5: Analysis of SoC estimation for EKF and CQKF.

Filter	**Drive Cycle**	$R^2(-)$	**MAE(%)**	**RMSE(%)**
EKF	UDDS	0.9961	1.6548	2.2583
	DST	0.9945	2.0024	2.7227
CQKF	UDDS	0.9969	1.4225	2.0023
	DST	0.9963	1.7531	2.1201

Table 6: Analysis of terminal voltage for EKF and CQKF.

Filter	**Drive Cycle**	$R^2(-)$	**MAE(mV)**	**RMSE(mV)**
EKF	UDDS	0.9244	11.1244	38.0012
	DST	0.8964	10.9365	37.9855
CQKF	UDDS	0.9165	10.8067	36.1278
	DST	0.8998	10.0836	35.9856

In summary, the errors are less for the CQKF which concludes that the estimates provided by it are more accurate compared to those provided by the EKF. The reason is that the CQKF is more accurate filter than the EKF. As has been comprehensively discussed in Refs. [20, 21] that the EKF handles the non-linearity by considering only the first order Taylor series expansion. Therefore, the approximation poorly realizes the nonlinearities for highly nonlinear system. The CQKF, on the other hand, more accurately realizes the nonlinearity by using the quadrature rule, which in turn improves the filtering performance. Please refer to [20, 21] for a detail discussion on implementing the CQKF and EKF filtering algorithms.

5 Conclusion

The SoC estimation of Li-ion cells is crucial in EV technologies. The complexity and nonlinearity are increasing in BMS. As the EKF algorithm could not handle the high parametric modeling uncertainties, using proper initialization and tuning can give a good estimate result. In this work, we implement the CQKF algorithm to handle high parametric uncertainty in BMS. Finally, the algorithms were tested using a real dataset. From the simulation results, it can be concluded that the CQKF outperforms EKF in the case of hard non-linearities and high parametric uncertainty. Considering the fact that EKF is simpler with fewer computational demands, the choice of estimation algorithms should be based on the battery's operating conditions. Also, it is better to obtain the parameters of the battery using a real-time drive cycle, if the application of these battery cells will be used in electric vehicles. For future work, the temperature effect on SoC estimation as well as aging and capacity estimation can be considered.

It should be noted that the noises considered in the paper are zero-mean Gaussian distribution, which holds for a range of practical battery systems. However, in certain battery systems, the noises appearing in the system model may follow non-Gaussianity. In such cases, the state-space model of the cell can be rederived to account for the non-Gaussian noises. Accordingly, the CQKF can be reformulated, which in the present form is structured only for Gaussian noise. It leaves a space for a promising future research direction.

Author contributions

Shivam Gupta: Conceived and designed the analysis, Collected the data, Contributed data or analysis tools, Performed the analysis, Wrote the paper.

Amit Kumar Naik: Contributed data or analysis tools, Performed the analysis, Wrote the paper.

Rajeeb Dey: Conceived and designed the analysis, Contributed data or analysis tools, Wrote the paper, Editing & organization of the manuscript.

Abhinoy Kumar Singh: Conceived & designed the analysis, Performed the analysis, Wrote the paper, Editing & reorganization of the manuscript.

Mihaela Popa: Conceived & designed the analysis, Performed the analysis, Wrote the paper, Editing & reorganization of the manuscript.

Alexandru Popa: Conceived & designed the analysis, Performed the analysis, Wrote the paper, Editing & reorganization of the manuscript.

Conflict of interest

The authors declare no conflict of interest.

References

[1] L. Lu, X. Han, L. Jianqiu, J. Hua, and M. Ouyang, "A review on the key issues for lithium-ion battery management in electric vehicles," *J. Power Sources*, vol. 226, p. 272–288, 03 2013.

[2] W. Li, Y. Xie, X. Hu, Y. Zhang, H. Li, and X. Lin, "An online SOC-SOTD joint estimation algorithm for pouch li-ion batteries based on spatio-temporal coupling correction method," *IEEE Trans. Power Electron*, vol. 37, no. 6, pp. 7370–7386, 2021.

[3] G. L. Plett, *Battery Management Systems, Volume I: Battery Modeling.* Artech House, 2015.

[4] ——, *Battery Management Systems, Volume II: Equivalent-Circuit Methods.* Artech House, 2015.

[5] J. Klee Barillas, J. Li, C. Günther, and M. A. Danzer, "A comparative study and validation of state estimation algorithms for li-ion batteries in battery management systems," *Appl. Energy*, vol. 155, pp. 455–462, 2015.

[6] B. Fridholm, M. Nilsson, and T. Wik, "Robustness comparison of battery state of charge observers for automotive applications," *IFAC Proc. Volumes*, vol. 47, no. 3, pp. 2138–2146, 2014, 19th IFAC World Congress.

[7] P. Saha, S. Dey, and M. Khanra, "Modeling and state-of-charge estimation of supercapacitor considering leakage effect," *IEEE Trans. Ind. Electron.*, vol. 67, no. 1, pp. 350–357, 2020.

[8] C. Campestrini, T. Heil, S. Kosch, and A. Jossen, "A comparative study and review of different Kalman filters by applying an enhanced validation method," *J. Energy Storage*, vol. 8, pp. 142–159, 11 2016.

[9] Y. Wang, C. Li, Q. Sun, and Y. Chang, "Research on SOC estimation of lithium-ion batteries based on robust full order proportional integral observer," *Int. J. Electrochem. Sci.*, p. 100645, 2024.

[10] J. Li, G. Bai, J. Yan, and J. Gu, "On-line parameter identification and SOC estimation of nonlinear model of lithium-ion battery based on wiener structure," *J Energy Storage*, vol. 92, p. 112094, 2024.

[11] G. Plett, "Extended Kalman filtering for battery management systems of lipb-based hev battery packs," *J. Power Sources*, vol. 134, pp. 262–276, 08 2004.

[12] ——, "Sigma-point Kalman filtering for battery management systems of LiPB-based HEV battery packs," *J. Power Sources*, vol. 161, pp. 1356–1368, 10 2006.

[13] X. Hu, S. Li, and H. Peng, "A comparative study of equivalent circuit models for Li-ion batteries," *J. Power Sources*, vol. 198, p. 359–367, 01 2012.

[14] C. Campestrini, M. Horsche, I. Zilberman, T. Heil, T. Zimmermann, and A. Jossen, "Validation and benchmark methods for battery management system functionalities: State of charge estimation algorithms," *J. Energy Storage*, vol. 7, pp. 38–51, 08 2016.

[15] B. Fridholm, T. Wik, and M. Nilsson, "Robust recursive impedance estimation for automotive lithium-ion batteries," *J. Power Sources*, vol. 304, pp. 33–41, 02 2016.

[16] A. A. Tayeb, R. W. Aldhaheri, and M. S. Hanif, "Vehicle speed estimation using gaussian mixture model and kalman filter," *International Journal of Computers Communications & Control*, vol. 16, no. 4, 2021.

[17] Z. Wu, M. Huang, Z. Xing, and T. Yang, "Improving short-term traffic flow prediction using grey relational analysis for data filtering and stacked lstm modeling," *International Journal of Computers Communications & Control*, vol. 19, no. 1, 2024.

[18] R. E. Kalman, "A new approach to linear filtering and prediction problems," 1960.

[19] R. G. Brown, P. Y. Hwang *et al.*, *Introduction to random signals and applied Kalman filtering.* Wiley New York, 1992, vol. 3.

[20] A. K. Singh, "Major development under Gaussian filtering since unscented Kalman filter," *IEEE/CAA Jr. Autom. Sinica*, In press.

[21] S. Bhaumik and P. Date, *Nonlinear estimation: methods and applications with deterministic Sample Points.* CRC Press, 2019.

[22] X. Zhao, B. Sun, W. Zhang, X. He, S. Ma, J. Zhang, and X. Liu, "Error theory study on EKF-based SOC and effective error estimation strategy for li-ion batteries," *Appl. Energy*, vol. 353, p. 121992, 2024.

[23] A. K. Singh, M. V. Rebec, and A. Haidar, "Kalman-based calibration algorithm for agamatrix continuous glucose monitoring system," *IEEE Trans. Control Syst. Technol.*, vol. 29, no. 3, pp. 1257–1267, 2021.

[24] H. Perez, J. Siegel, X. Lin, A. Stefanopoulou, Y. Ding, and M. Castanier, "Parameterization and validation of an integrated electro-thermal cylindrical lfp battery model," vol. 3, 10 2012.

[25] X. Lin, H. Perez, J. Siegel, and A. Stefanopoulou, "An Electro-thermal Model for the A123 26650 LiFePO4 Battery," 04 2013.

[26] S. Hossain Ahmed, X. Kang, and S. Bade Shrestha, "Effects of temperature on internal resistances of lithium-ion batteries," *Journal of energy resources technology*, vol. 137, no. 3, 2015.

[27] S. Bhaumik and Swati, "Cubature quadrature Kalman filter," *IET Signal Process.*, vol. 7, pp. 533–541, 09 2013.

[28] E. Vergori, F. Mocera, and A. Somà, "Battery modeling and simulation using a programmable testing equipment," in *2017 9th Computer Science and Electronic Engineering (CEEC)*, 2017, pp. 162–167.

Journal's webpage: http://univagora.ro/jour/index.php/ijccc/

This journal is a member of, and subscribes to the principles of,
the Committee on Publication Ethics (COPE).
https://publicationethics.org/members/international-journal-computers-communications-and-control

Cite this paper as:

Gupta, S.; Naik, A.K.; Dey, R.; Singh, A. K.; Popa, M.; Popa, A. (2025). State-of-Charge Estimation of an Experimentally Identified Lithium-ion Cell Model using Advanced Nonlinear Filters, *International Journal of Computers Communications & Control*, 20(2), 6896, 2025.
https://doi.org/10.15837/ijccc.2025.2.6896